Traffic Reduction in Packet Switched Networked Control Systems using Deadband Error Modulation

Upeka Premaratne, Saman K. Halgamuge and Iven M. Y. Mareels

***Abstract*—This paper introduces a novel traffic reduction method for Networked Control Systems (NCS) called Deadband Error Modulation (DEM). The deadband modifies the periodic dynamics of Delta Modulation (DM) based techniques such as our previously proposed Event Triggered Adaptive Differential Modulation (ETADM). Like ETADM it can be used for encoding individual scalar elements of a vector (i.e., the state vector or control input). It is also robust to bounded packet drops.**

***Keywords*—Networked control systems, network traffic reduction, speech coding, deadband error modulation**

I. Introduction

Congestion in a communication network is a major cause of packet drops [1]. This occurs due to queues being unable to accept packets after they have reached capacity (i.e., tail drop). Despite the technical advances that result in increased bandwidth [2], emerging trends such as seamless integration of enterprise and automation networks [3] and Internet of Things (IoT) [4] where more and more entities are networked, result in increased utilization of the available bandwidth. A two pronged approach can be taken to solve this with one being optimizing the network topology to reduce congestion. The other possibility is to reduce traffic generated by the sensors, controllers and actuators of the Networked Control System (NCS). Due to the large packet overhead of packet switched communication networks, reducing the size of the transmitted data is inefficient. Instead, the viable solution is to reduce network traffic by reducing the effective sampling rate.

A. Contribution

In this paper we propose a new method of reducing traffic in NCS called Deadband Error Modulation (DEM). The inspiration for this new method comes from our previously proposed Event Triggered Adaptive Differential Modulation (ETADM) [5] which combines Speech Coding (SC) techniques and event based sampling. DEM has a simpler implementation and traffic reduction capability that exceeds ETADM.

B. Comparison with Previous Work

Compared to previously proposed methods that use derivatives of Adaptive Delta Modulation (ADM) [6] [7], DEM differs in many respects. In both [6] [7], a single encoded bit is transmitted across the communication network for every periodic sample of the sensor and stability is proven only for a linear plant. Due to the step adaptation at the decoder (Fig. 2 of [7] and implicitly mentioned in Fig. 6 of [6]) both are vulnerable to packet drops. Hence, a synchronization protocol has to be executed (after receiving a predetermined number of similar consecutive transmitted symbols) to recover from a possible packet drop [7] (this is not discussed in [6]). In both papers the communication channel is assumed to be 100% reliable (i.e., without loss of transmitted data) and delay free.

In DEM, the deadband alters the dynamics of the encoder significantly compared to ADM. In the ETADM encoder of [5], the sign function used for the step adaptation is such that $sgn(0) = 0$. Thus, when the error between the input and encoder reconstruction e_i (6) is zero, the encoder output is zero and no data needs to be transmitted. However, under noisy conditions the likelihood of $e_i = 0$ is almost negligible because a small perturbation would make $e_i \neq 0$ and the output of the sign function ± 1. In DEM the deadband solves this by making the encoder output zero for $|e_i| \leq d_0$ where d_0 is the deadband width (Fig. 2). Thus, when $|e_i| \leq d_0$ the DEM encoder stays in this transmission free state for a significant duration until $|e_i| > d_0$ due to attenuation of the lossy integrator output.

According to Section I-E of [6] $sgn(0)$ is arbitarily assigned ± 1. Similarly in [7] from the same authors the value of the sign function is encoded to a binary digit (i.e., only $\pm$). Hence, the transmission free state correspoding to $e_i = 0$ does not exist in the ADM encoders of [6] and [7].

Thus, the deadband in a DEM encoder makes the communication channel use sporadic (aperiodic) compared to periodic in [6] [7] resulting in a reduction in the *effective sampling rate* (i.e., traffic rate) (27). This makes it more suitable for packet switched communication networks due to the reduction of packet transmissions. There is also no independent adaptation of the step size in the DEM encoder and decoder which makes it inherently robust to bounded packet drops compared to [7]. From Lemma 3 the local stability of a control loop using DEM encoding is established for nonlinear plants with a bounded delay using Razumikhin type theorems [8]. DEM also outperforms Memory Based Event Triggering (MBET) [9] [10] [11] for the given simulated example.

C. Outline of this Paper

The main results of this paper are discussed in Section III. These results include the dynamics of DEM encoders and the stability of control systems with DEM encoding. The traffic reduction methods are compared using a simulated linear plant with a saturating actuator in Section IV.

U. Premaratne is with the Department of Electronic and Telecommunication Engineering, University of Moratuwa, Katubedda, Moratuwa 10400, Sri Lanka e-mail:upeka@uom.lk

S. Halgamuge is with the Research School of Engineering, College of Engineering and Computer Science, the Australian National University, Canberra, ACT 2601, Australia e-mail: saman.halgamuge@anu.edu.au

I. Mareels is with the Department of Electrical and Electronic Engineering, the University of Melbourne, Parkville, VIC 3010, Australia e-mail: i.mareels@unimelb.edu.au

The authors acknowledge the support from Australian Research Council Linkage, Infrastructure, Equipment and Facility Grant LE120100117.

II. Preliminaries

A. Notations

The symbols $\mathbb{R}$ and $\mathbb{Z}^+$, represent the set of real numbers and positive integers (excluding zero) respectively. A subscript $i \in \mathbb{Z}^+$ such as in v_i denotes a scalar element of a vector $v = [\ v_1 \quad v_2 \quad \dots \quad v_n\ ] \in \mathbb{R}^n$ or a scalar in general. The Euclidean and standard L_P norms of a vector v are given by $|v|$ and $||v||_p$ respectively unless stated otherwise. For v_i, the norm $|v_i|$ is simply the absolute value.

The letters $\mathcal{K}$, $\mathcal{K}_\infty$ and $\mathcal{KL}$ represent the class of functions as defined in [12] (p. 144). For two functions $f, g \in \mathcal{K}$, $f \circ g(r) := f(g(r))$. The function definition $sgn(r)$ denotes the sign function where $sgn(0) = 0$, $sgn(r) = 1$ when $r > 0$ and $sgn(r) = -1$ when $r < 0$.

The letter $k \in \mathbb{Z}$ in square brackets is used for periodic (clocked) discrete time signals unless stated otherwise. The overbar ($\bar{v}$) on a variable represents its reconstruction.

The state of a DEM encoder is denoted by $X \in \mathcal{X} = \{S_-, Z, S_+\}$. Uppercase letters are used to indicate an encoder state and make the distinction from the scalar encoder input x_i. For a particular encoder state a subscript of the form X_k denotes the state at time k and a state transition is represented by $X_k \rightarrow X_{k+1}$. The notation $(X)_n$ is used to denote n consecutive transitions where the encoder state X remains unchanged. For n consecutive repetitions of a transitions of the form $Y \rightarrow X$ (i.e., $Y \rightarrow X \rightarrow Y \rightarrow \cdots \rightarrow X$), the notation $(Y \rightarrow X)_n$ is used (where $Y \in \mathcal{X}$). A cycle that starts at state X is denoted by $X \rightarrow \cdots \rightarrow X$. The notation C_{X_{k+1}/X_k} indicates the conditions for the transition $X_k \rightarrow X_{k+1}$.

B. Control System Model

Consider an autonomous plant with continuous dynamics described by,

$$\dot{x} \quad = \quad f(x, u, w) \tag{1}$$

where $x \in \mathbb{R}^{n_x}$ is the system state, $u \in \mathbb{R}^{n_u}$ the control input and $w \in \mathbb{R}^{n_w}$ an exogenous disturbance. $n_x, n_u, n_w \in \mathbb{Z}^+$. $f(x, u, w)$ is Lipschitz in x, u and w for $(x, u, w) \in \Omega \subseteq \mathbb{R}^{n_x} \times \mathbb{R}^{n_u} \times \mathbb{R}^{n_w}$. The origin of (1) is an equilibrium point; $f(0, 0, 0) = 0$.

Assumption 1. *x is measurable.*

Assumption 2. *There exists a stabilising control law $u = \phi(x)$ such that $\dot{x} = f(x, \phi(x)+e, w)$ is locally Input to State Stable (ISS) from w, e to x, where e is the network induced error.*

Therefore, from (8) of [13] there exists a C^1 Lyapunov function $V : D \rightarrow \mathbb{R} \geq 0$ and $\alpha_1, \alpha_2, \alpha_3, \rho_e, \rho_w \in \mathcal{K}$ such that for a network induced error e,

$$\alpha_1(|x|) \leq V(x) \leq \alpha_2(|x|), \tag{2}$$

$$\dot{V} = \frac{\partial V}{\partial x} f(x, \phi(x) + e, w), \tag{3}$$

$$|x| \quad \geq \quad \rho_e(|e|) \vee \rho_w(|w|) \Rightarrow \dot{V} \leq -\alpha_3(|x|). \tag{4}$$

Assumption 3. *For the sampling time T_S there exists an error bound Δ_q where $|x_i(t) - x_i[k]| \leq \Delta_q$ for $t \in [(k-1)T_S, kT_S)$. For convenience, Δ_q is taken as the upper bound of the quantization error.*

Assumption 4. *All sensors, the controller and the plant have ideal synchronized clocks for periodic sampling and reconstruction.*

Assumption 5. *The communication network uses packet switched multiple access with a negligible channel access time compared to the periodic sampling rate.*

From Assumption 3, (1) need not be considered as a discrete system for stability analysis as in [14]. Assumptions 4 and 5 are necessary to neglect any effect due to delay variation (jitter).

III. Main Results

A. The DEM Encoder

In the control system that satisfies Assumptions 1 and 5, DEM encoders (Fig. 1) are used to encode individual scalar elements of x and u. Let the state space representation of the encoder be given by,

$$\bar{x}_i[k+1] = K\bar{x}_i[k] + K\Phi(x_i[k] - \bar{x}_i[k]) \tag{5}$$

where Φ is defined as a piecewise continuous function for $e_i[k]$ which is the error between the scalar encoder input $x_i[k]$ and reconstruction $\bar{x}_i[k]$ such that,

$$e_i[k] = x_i[k] - \bar{x}_i[k]. \tag{6}$$

The output, $s_i[k] = \Phi(e_i[k])$. If $s_i[k] \neq 0$, it is encoded into a single packet and transmitted across the channel to the destination where the signal is reconstructed by a second lossy integrator (i.e., the decoder).

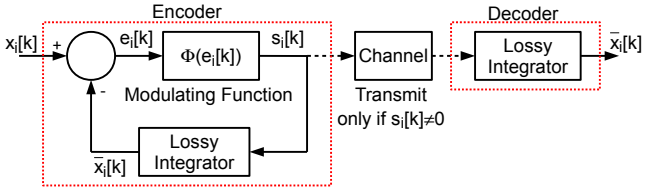

Fig. 1. Implementation of a DEM Encoder

The modulation function (Fig. 2) can be defined such that,

$$s_i[k] = \begin{cases} 0 & |e_i[k]| \leq d_0 \\ s_0 sgn(e_i[k]) & d_0 < |e_i[k]| \end{cases} \tag{7}$$

so that it consists of a deadband between $\pm d_0$ and a saturation region beyond $\pm d_0$. When compared to a scalar variable at the source periodically sampled and transmitted across the network to the destination, the additional hardware needed for DEM are the encoder and decoder. The additional computational steps are the encoding, modulation and decoding of the variable by (5), (7) and (8) respectively.

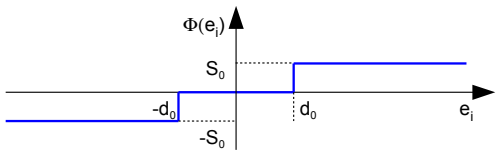

Fig. 2. Modulating Function for DEM Encoding

B. DEM Encoder Dynamics

The hybrid dynamics of the encoder consist of three discrete states depending on the region of the modulation function (7). They are defined as the deadband state Z and the saturated states for $\pm e$ (S_+ and S_- respectively). A function of form (7), has a minimal number of states (compared to the ETADM encoder of [5]) and makes (5) ISS for all of them.

The transfer function of the lossy integrator is given by,

$$H(z) \quad = \quad \frac{Kz^{-1}}{1-Kz^{-1}}. \tag{8}$$

For the integrator to be stable without oscillations, $0 < K < 1$. The reconstructed signal is given by,

$$\bar{x}_i[k+1] \quad = \quad \sum_{j=0}^{k} K^{k-j+1} s_i[j] + K^{k+1}\bar{x}_i[0]. \tag{9}$$

The state transitions of a DEM encoder can be represented by Fig. 3. The conditions for each state transition are given in Table I. The notation C_{X_{k+1}/X_k} indicates the conditions for the transition $X_k \rightarrow X_{k+1}$. Due to the finite number of states and transitions of Fig. 3 with unambiguous conditions for triggering each state transition (Table I), the occurrence of chaotic dynamics can be excluded.

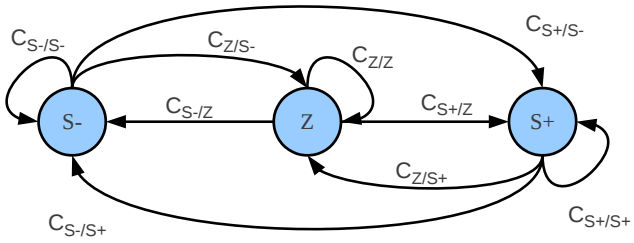

Fig. 3. DEM Encoder State Transitions

TABLE I. DEM ENCODER STATE TRANSITION CONDITIONS

Transition	Condition
$X \rightarrow Z$ where $X = Z, S_-, S_+$	$\lvert x - \bar{x}_i \rvert \leq d_0$
$Z \rightarrow S_+$ and $S_+ \rightarrow S_+$	$x - \bar{x}_i > d_0$
$Z \rightarrow S_-$ and $S_- \rightarrow S_-$	$x - \bar{x}_i < d_0$
$S_+ \rightarrow S_-$ and $S_- \rightarrow S_+$	Overshoot conditions (15) and (16)

From (8), the lossy integrator input can either assist the attenuation when $\bar{x}_i[k+1] = K\bar{x}_i[k] - Ks_i[k]$, or oppose the attenuation $\bar{x}_i[k+1] = K\bar{x}_i[k] + Ks_i[k]$ where $sgn(\bar{x}_i[k]) = sgn(s_i[k])$. Depending on the state of e_i and sign of $\bar{x}_i[k]$, this attenuation state of the lossy integrator can be summarized according to Table II. Attenuation assistance occurs if

$$sgn(x_i[k]) \quad = \quad -sgn(\bar{x}_i[k]) \tag{10}$$

or

$$\left.\begin{array}{c} sgn(x_i[k]) = sgn(\bar{x}_i[k]) \\ |e_i[k]| > d_0 \\ |\bar{x}_i[k]| > |x_i[k]| \end{array}\right\} \tag{11}$$

Within the deadband the encoder dynamics reduce to,

$$\bar{x}_i[k+1] \quad = \quad K\bar{x}_i[k] \tag{12}$$

and the reconstruction will gradually attenuate until it exits the deadband.

TABLE II. LOSSY INTEGRATOR ATTENUATION STATE SUMMARY

e_i	DEM Encoder State	Attenuation State	
		$\bar{x}_i[k] > 0$	$\bar{x}_i[k] < 0$
$> d_0$	S_+	Opposing	Assisting
$< -d_0$	S_-	Assisting	Opposing

The necessary conditions for $\bar{x}_i$ to converge to a constant encoder input $x_i[k] = x_C$ are obtained in Theorem 1. The subsequent asymptotic behavior and error bound is obtained from Theorem 2. Lemma 2 proves that Theorem 2 continues to hold for a variable encoder input with high dependence. For an encoder input that varies beyond the bound of Lemma 2, the DEM encoder will re-converge to it. Sample reconstructions of DEM (Fig. 4) are provided for the reader to get an intuitive idea of this encoding method.

Theorem 1. *The DEM encoder of (5) with modulation function, $\Phi(e_i[k])$ defined by (7) with encoder states Z ($|e_i[k]| \leq |d_0|$), S_+ ($e_i[k] > d_0$) and S_- ($e_i[k] < -d_0$), where $\pm d_0$ is the deadband zone of $\Phi(e_i[k])$, $e_i[k]$ is the reconstruction error $x_i[k] - \bar{x}_i[k] = e_i[k]$ for the scalar encoder input $x_i[k]$ and reconstruction $\bar{x}_i[k]$, will converge to within the deadband for a constant encoder input $x_i[k] = x_C$ if and only if $|x_C| < d_0 + \frac{K}{1-K}s_0$.*

Proof: For an arbitrary constant encoder input x_C and initial reconstruction $\bar{x}_i[0]$, such that $|e_i[0]| > d_0$, $s_i[k] = \pm s_0$. Therefore, the transition $X_k \rightarrow X_{k+1}$ will occur where $X_{k+1} = X_k = S_+$ (or S_-).

If $\bar{x}_i[k]$ is to converge to x_C,

$$\begin{aligned} |x_C - \bar{x}_i[0]| \quad &> \quad \cdots > |x_C - \bar{x}_i[k]| \\ &> |x_C - \bar{x}_i[k+1]| > \ldots . \end{aligned} \tag{13}$$

When the lossy integrator is under assisted attenuation due to condition (11), convergence to x_C is trivial. Condition (10) will result in opposing attenuation once $sgn(x_i[k]) = sgn(\bar{x}_i[k])$. When the input of the lossy integrator opposes attenuation, for (13) to converge $|\bar{x}_i[k+1]| > |\bar{x}_i[k]|$. This occurs when,

$$|\bar{x}_i[k]| < \frac{K}{1-K}s_0. \tag{14}$$

If $|\bar{x}_i[0]| \geq \frac{K}{1-K}s_0$, from (9) when $k \rightarrow \infty$, the initial value will attenuate; resulting in (14) and convergence.

From Fig. 3, the converging DEM encoder can remain in S_+ or S_- until it enters the deadzone or overshoots (and subsequently enters the deadzone). For brevity the proof for exceptional overshoots (Remark 1) is omitted.

In either case to converge to within the deadband $|x_C - \bar{x}_i[k]| \leq d_0$. Hence, $|x_C| \leq d_0 + |\bar{x}_i[k]| < d_0 + \frac{K}{1-K}s_0$. ■

Remark 1. *For no overshoots to occur, the parameters Δ_O and Δ_A given by*

$$\Delta_O \quad = \quad Ks_0 - (1-K)|\bar{x}_i[k]| - 2d_0, \tag{15}$$

$$\Delta_A \quad = \quad Ks_0 + (1-K)|\bar{x}_i[k]| - 2d_0 \tag{16}$$

with $sgn(s_i[k]) = sgn(\bar{x}_i[k]$ have to be $\Delta_O, \Delta_A \leq 0$ for all $\bar{x}_i[k] \in \left(-\frac{K}{1-K}s_0, \frac{K}{1-K}s_0\right)$. The conditions account for overshoots under opposing (15) and assisting (16) attenuation.

Lemma 1. *For a constant encoder input $x_i[k] = x_C$, if $0 \notin [x_C - d_0, x_C + d_0]$, a DEM encoder of (5) with modulation function, $\Phi(e_i)$ defined by (7) at state Z (i.e., in*

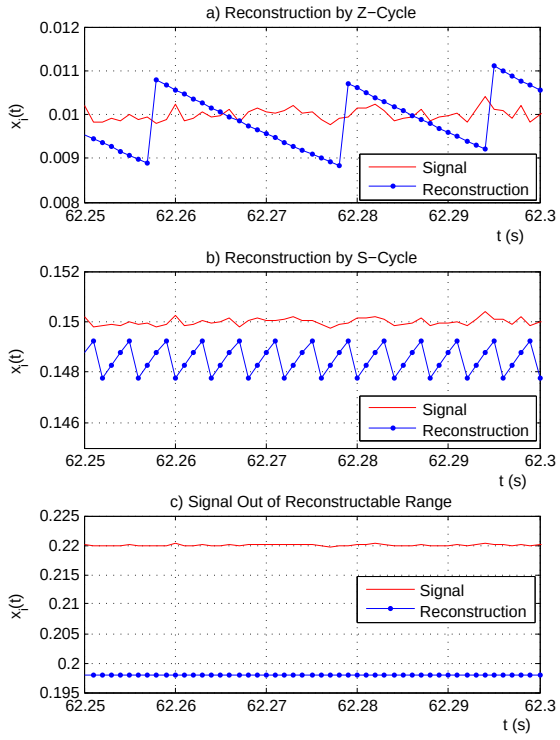

Fig. 4. Sample DEM Signal Reconstruction

the deadband) will only undergo state transitions such that $sgn(\bar{x}_i[k]) = sgn(s_i[k])$ *when exiting the deadband.*

Proof: From the attenuation within the deadzone (12), when exiting $|x_C| > |\bar{x}_i[k]|$. Thus, when $x_C > \bar{x}_i[k] > 0$, $e_i[k] > d_0$, resulting in only $Z \to S_+$. Similarly for $x_C < \bar{x}_i[k] < 0$, $e_i[k] < -d_0$, the only possible transition is $Z \to S_-$. Therefore, when exiting the deadband, the state transition must satisfy $sgn(\bar{x}_i[k]) = sgn(s_i[k])$. ■

Corollary 1. *If the DEM encoder overshoots after exiting the deadzone, it can only be due to an opposing overshoot (15).*

Theorem 2. *For a constant encoder input* $x_i[k] = x_C$*, once the reconstruction* $\bar{x}_i[k]$ *of the DEM encoder of (5) with modulation function* $\Phi(e_i[k])$ *defined by (7), reaches the deadband (i.e., the DEM encoder state becomes Z), it will continue as an asymptotic periodic cycle with a reconstruction error* $|e_i[k]| < Ks_0 + d_0$.

Proof: Once in the deadband from (12), $\bar{x}_i$ will attenuate until it exits the deadband satisfying the condition of Lemma 1. For convenience we will take X_k of the transition $Z_{k-1} \to X_k$ as the first value of the periodic cycle and corresponding value of $\bar{x}_i[k] = \bar{x}_S$ and $s_i[k] = s_I$ such that $sgn(\bar{x}_S) = sgn(s_I)$ (Lemma 1).

In DEM an asymptotic periodic cycle with a period of p samples is when $\bar{x}_i[k+p] = \bar{x}_i[k] = \bar{x}_S$, resulting in the relationship

$$\sum_{j=k}^{k+p-1} K^{k+p-j} s_i[j] = (1-K^p)\bar{x}_S \tag{17}$$

From the DEM encoder state diagram (Fig. 3) three types of periodic cycles that satisfy (17) by a single cycle can occur:

1) Z-cycles of the form $X \to (Z)_n \to X$ (where $X = S_+$ or S_- and $n \geq 1$) where the dynamics are mainly within the deadband (Fig. 4a),
2) S-cycles where the dynamics are mainly within the saturation region and are of the form $Z \to (X)_n \to Z$ (where $X = S_+$ or S_- and $n \geq 1$) (Fig. 4b) and
3) O-cycles (overshoot cycles) of the form $(X \to Y)_n \to X \to (Z)_m \to X$ (where $X = S_\pm$, $Y = S_\mp$ and $m, n \geq 1$) when $\Delta_O > 0$ of (15) is satisfied.

When $n = 1$, the resulting periodic cycle can be classified as both a Z and S-cycle. These cycles will be subsequently referred to as simple asymptotic cycles because they can satisfy (17) in a single cycle as opposed to compound cycles that require multiple cycles to satisfy (17). Compound cycles are briefly explained in the Appendix.

For brevity we will limit this proof to Z-cycles due to their high efficiency. The generic relationship of (17) for a simple Z-cycle is given by

$$\bar{x}_S = \frac{K^p}{(1-K^p)} s_I \tag{18}$$

where $p = 2$ to ∞. Hence, $0 < K^p \leq K^2$. This results in a range for $\bar{x}_S$ of,

$$0 < |\bar{x}_S| \leq \frac{K^2}{1-K^2} s_0. \tag{19}$$

Therefore, a DEM encoder generates Z-cycles when $|\bar{x}_i|$ converges to a value under the threshold of $K^2 s_0/(1-K)$ and S-cycles when converging to a value above it. When approaching the bound of $Ks_0/(1-K)$, at the asymptote, the DEM encoder remains within one of the saturated states because from (17) $s_i[k+1] = s_i[k] = \pm s_0$ for all k.

For all cycles,

$$\bar{x}_S \in [Kx_{\min}, x_{\min}) \tag{20}$$

where $x_{\min} = (x_C - sgn(x_C)d_0)$. From the result of Theorem 1 and (20) $|e_i[k]| < Ks_0 + d_0$. ■

Remark 2. *The dynamics of O-cycles are similar to Z cycles but less efficient in terms of traffic reduction due to overshoots.*

Remark 3. *From (15), to ensure no overshoots occur for a Z-cycle for all values of* $\bar{x}_i$*,* $s_0 \leq 2d_0/K$*. The cycle with the longest period and least generated traffic occurs when,* $s_0 = 2d_0/K$*, making it the optimal set of parameters. K has to be made as close to unity as possible depending on the physical implementation.*

Lemma 2. *An asymptotic Z-cycle of a DEM encoder will be preserved for a variable encoder input* $x_i[k]$ *with high dependence.*

Proof: For an constant $x_i[k] = x_C$, consider the state transition $Z \to S_\pm$ when $|x_C - \bar{x}_i[k-1]| \leq d_0$ and $|x_C - \bar{x}_i[k]| = |x_C - \bar{x}_S| > d_0$ where $\bar{x}_S = K\bar{x}_i[k-1]$. This results in

$$|x_C - d_0| \in \left(\bar{x}_S, \frac{\bar{x}_S}{K}\right]. \tag{21}$$

Therefore, for a variable encoder input, there exists a sufficiently small bound λ_0 such that

$$|x_i[k] - x_i[k-1]| \leq \lambda_0 < \frac{d_\Delta}{2} < d_0 \tag{22}$$

and (21) is preserved where $d_\Delta = |\bar{x}_S|(1-K)/K$. Hence, if $x_i[k]$ varies in a highly dependent manner, the prevailing asymptotic Z-cycle will be preserved. ■

C. Stability Error Bounds

1) Packet Drop Error Bound: From Lemma 1 of [5], the bound on the error due to P consecutive packet drops (e_{D_i}) is given by,

$$|e_{D_i}| \leq \frac{(1-K^P)Ks_0}{1-K}. \tag{23}$$

If the probability of a packet drop is sufficiently small such that two packet drops within N samples is statistically improbable, $P = 1$.

2) Total Error Bound: From the result of Theorem 2 and (23), the total error bound for a single reconstructed variable Λ_i is given by,

$$\begin{aligned} |\Lambda_i| &\leq |e_i[k]| + |e_{D_i}| + \Delta_q \\ &\leq (Ks_0 + d_0) + \frac{(1-K^P)Ks_0}{1-K} + \Delta_q. \end{aligned} \tag{24}$$

From (24), it is possible to define a vector of error bounds $\Lambda = [\Lambda_1, \Lambda_2, \dots \Lambda_i \dots]^T$. In Section III-D, this error bound is used to establish the stability of the NCS.

D. Control System Stability

Stability of the NCS is established by proving the ISS of the continuous time system (Assumption 2) with respect to the disturbance, network delays and reconstruction error. The feedback path reconstructs the state $\bar{x}_i$ and control input $\bar{\phi}$ at a total delay of τ. Therefore, the control system would be given by,

$$\dot{x}(t) = f(x(t), \bar{\phi}(\bar{x}_i(t-\tau)), w(t)). \tag{25}$$

The network induced error e will consist of an error e_τ due to delay τ (bounded by a maximum time $\tau_{\max}$), an error e_x due to reconstruction of the state vector and an error e_u due to reconstruction of the control inputs. Therefore,

$$\begin{aligned} u &= \phi(x(t)) + e_\tau(t) + e_x(t) + e_u(t), \\ e_\tau(t) &= \phi(x(t-\tau)) - \phi(x(t)), \\ e_x(t) &= \phi(\bar{x}(t-\tau)) - \phi(x(t-\tau)), \\ e_u(t) &= \bar{\phi}(\bar{x}(t-\tau)) - \phi(\bar{x}(t-\tau)). \end{aligned} \tag{26}$$

The stability of the feedback loop is established by Theorem 1 of [5]. From the result of From Theorem 1, every individual scalar element of x or u that is encoded has an upper bound for convergence. Hence, it is necessary to establish a domain for which the entire vector (x, u) converges to ensure that the system (25) is ISS.

Lemma 3. *The dynamic system of (25) for which Assumptions 1 to 5 hold; when using DEM for signal reconstruction of individual elements of x and u is locally ISS for the domain $\mathcal{D} = \{v \in \mathbb{R}^{n_x} \times \mathbb{R}^{n_u} | \bigcup_{i=1}^{n_x+n_u} |v_i| \leq M_i\}$ where $v = (x, u)$ and M_i is the maximum value of individual element v_i for convergence.*

Proof: From Theorem 1 for all v_i of v there exists an upper bound $|v_i| \leq M_i$ for convergence depending on the parameters K, d_0 and s_0. When $|v_i| > M_i$ the DEM reconstruction error is unbounded since $v_i \in \mathbb{R}$. For any i, if e_i is unbounded, (24) will become unbounded. Thus, from Theorem 1 of [5] ([8]), the solution of (25) cannot be ultimate bounded. Therefore, the system (25) can only be ISS for the domain $\mathcal{D} = \{v \in \mathbb{R}^{n_x} \times \mathbb{R}^{n_u} | \bigcup_{i=1}^{n_x+n_u} |v_i| \leq M_i\}$. ■

Remark 4. *The domain $\mathcal{D}$ is a hyper-rectangle around the origin with the length along dimension v_i being $2M_i$. In the special case when the parameters K, d_0 and s_0 are identical for all i, the domain $\mathcal{D} = \left\{v \in \mathbb{R}^{n_x} \times \mathbb{R}^{n_u} | \|v\|_\infty \leq d_0 + \frac{K}{1-K} s_0\right\}$.*

IV. Simulation Results

In this section DEM is tested on a Simulink model of the nonlinear ship roll stabilizer (Fig. 5) of [5]. To the best of the authors' knowledge a formal method of comparing the traffic reduction does not exist due to the unquantifiable possibilities of input signal shapes and input noise. Hence, a reasonable empirical comparison has to be made.

The simulated control system attenuates a bounded disturbance ($w \leq 0.3$) due to lateral waves on a linear ship hull using a saturating (i.e., nonlinear) stabilizing fin. In the simulated scenario, the tilt sensor is assumed to be located at a distance from the stabilizing fins and the reading from the sensor is encoded before transmission over the communication network. For the slow damping hull dynamics reasonable numerical values are selected: $K_0 = 4$, $a = 0.35$, $b = 4$ and for the actuator $|sat(r)| \leq 0.31$. For a maximum network delay of $4ms$ (4 samples) a gain (K_G) of 20 is used to maintain stability. The simulation is run for 100s totaling 100,000 samples. The ship is subject to a periodic tilting wave disturbance of 0.2 rad (11.5^o).

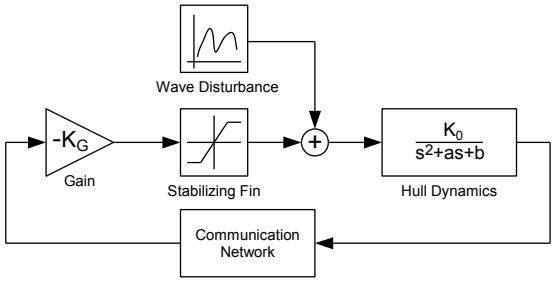

Fig. 5. Ship Roll Stabilizer - Control System

Depending on the encoder type (DEM, MBET and ETADM) and parameters, four systems are simulated (Table III) with K=0.9999 for both DEM and ETADM. They are compared in terms of generated traffic, reconstruction error and disturbance attenuation for delays of zero, 2ms and 4ms. In the benchmark system with periodic sampling, a single packet with the measured plant output is transmitted for each periodic sample. According to the simulation result, the measured value is encoded into a 64 bit double precision floating point number. In MBET, the transmitted value is 64 bits while in DEM and ETADM is encoded into a 8 bit value. In all three cases, a single packet is transmitted per encoded sample. The performance metric (i.e., traffic reduction) is obtained from

$$\eta = 100\left(1 - \frac{n_E}{n_B}\right) \tag{27}$$

where n_E and n_B are the number of packets generated by the encoding scheme and benchmark respectively. For this simulation $n_B = 100,000$.

TABLE III. SHIP ROLL STABILIZER - ENCODER PARAMETERS

Encoder	Parameters
ETADM	$S_{\min} = 0.01, S_{\max} = 0.04, \Delta S = 0.005$
MBET	$e_T = 0.01$
DEM	$s_0 = 2d_0 = 0.01$

TABLE IV. SHIP ROLL STABILIZER - PERFORMANCE COMPARISON

Delay (ms)	Encoder	Traffic Reduction		e_{RMS}	Attn. (dB)
		Packets	(%) Red.		
0	Bench	-	-	-	25.29
	ETADM	16600	83.40	0.0051	23.04
	MBET	2146	97.85	0.0057	7.58
	DEM	**592**	**99.41**	**0.0029**	**23.32**
2	Bench	-	-	-	22.08
	ETADM	17456	82.54	0.0052	**19.79**
	MBET	2159	97.84	0.0061	7.41
	DEM	**791**	**99.21**	**0.0028**	19.67
4	Bench	-	-	-	17.24
	ETADM	15565	84.43	0.0050	**17.43**
	MBET	2274	97.73	0.0066	6.45
	DEM	**1131**	**98.87**	**0.0029**	16.50

From the results (Table IV), DEM performs better than MBET in all three criteria. DEM also performs better than ETADM with the exception of disturbance attenuation for 2ms and 4ms delays. This along with the decreased transient response time from equation (27) of [5], are the two shortcomings of DEM compared to ETADM.

In order to illustrate the benefit of an encoder to reduce traffic, the samples generated by each encoder for the zero delay case are subject to a packet drop probability of 0.01 using a simulated Bernoulli random number generator. The results (Table V) clearly illustrate the reduction in packet drops. When compared with the benchmark, DEM reduces the number of packet drops from 971 to 6; resulting in a packet drop reduction of 99.38%.

TABLE V. PACKET DROP COMPARISON (ZERO DELAY CASE)

Encoder	No. of Samples	No. of Drops	(%) Red.
Benchmark	100000	971	-
ETADM	16600	168	82.70
MBET	2146	20	97.94
DEM	592	6	99.38

V. CONCLUSIONS

In this paper, DEM, a new method for reducing traffic in networked control systems is proposed. It is an improvement over previously proposed ETADM. In ETADM (from Theorem 3 of [5]), the lowest step size is blocked. This reduces network traffic by blocking the asymptotic periodic cycle to which the ETADM encoder converges to. In DEM the period of the asymptotic periodic cycle is lengthened by a deadband. Due to the use of a lossy integrator for signal reconstruction, DEM is robust to bounded packet drops like ETADM. The main future direction for this work is to further investigate the issues involved with implementing DEM on embedded systems. These include quantization, finite word lengths and floating point calculations. Investigating the applicability of DEM to systems with interconnected subsystems is another interesting future direction.

APPENDIX

Let $\epsilon = \epsilon_Z, \epsilon_S > 0$ be the minimum transitional difference of the DEM encoder where ϵ_Z and ϵ_S are the corresponding values for Z-cycles and S-cycles respectively. This results in,

$$\epsilon_Z = \min\left[(1-K)|\bar{x}_i[k]|\right] \;\; k \in \mathcal{K}_Z \tag{28}$$

$$\epsilon_S = \min\left[(K-1)|\bar{x}_i[k]| + Ks_0\right] \;\; k \in \mathcal{K}_S \tag{29}$$

Consider a cycle with a small offset δ_j such that $\bar{x}_i[k + jp] = \bar{x}_i[k] + \delta_j$ where $sgn(\delta_j) = sgn(\bar{x}_i)$ and $0 < |\delta_j| < \epsilon$. Taking $\bar{x}_i[k] = \bar{x}_S$, the cumulative offset for n such cycles can be expressed as,

$$\bar{x}_i[k + pn] = \bar{x}_S + \sum_{j=1}^{n} \delta_j. \tag{30}$$

For a sustained a periodic cycle, the term $\sigma = \sum_{j=1}^{n} \delta_j$ has to be eliminated. The resulting compound cycles, either add or omit a transition to compensate for σ. For example, $(X \to (Z)_p)_{n-1} \to X \to (Z)_{p+1} \to X$ and $(X \to (Z)_p)_{n-1} \to X \to (Z)_{p-1} \to X$.

REFERENCES

[1] H. Wu, Z. Feng, C. Guo, and Y. Zhang, "ICTCP: incast congestion control for tcp in data-center networks," *IEEE/ACM Transactions on Networking (TON)*, vol. 21, no. 2, pp. 345–358, 2013.

[2] T. S. Rappaport, R. W. Heath Jr, R. C. Daniels, and J. N. Murdock, *Millimeter wave wireless communications*. Pearson Education, 2014.

[3] J. Kirsch, S. Goose, Y. A. W. Dong, and P. Skare, "Survivable SCADA via intrusion-tolerant replication," *Smart Grid, IEEE Transactions on*, vol. 5, no. 1, pp. 60–70, 2014.

[4] S. Aleksic, G. Franzl, T. Bogner, and O. Mair am Tinkhof, "Framework for evaluating energy efficiency of access networks," in *Communications Workshops (ICC), 2013 IEEE International Conference on*. IEEE, 2013, pp. 548–553.

[5] U. Premaratne, S. K. Halgamuge, and I. M. Y. Mareels, "Event triggered adaptive differential modulation: A new method for traffic reduction in networked control systems," *IEEE Transactions on Automatic Control*, vol. 58 (7), pp. 1696–1706, 2013.

[6] C. Canudas-de-Wit, F. Gomez-Estern, and F. R. Rubio, "Delta-modulation coding redesign for feedback controlled systems," *IEEE Transactions on Industrial Electronics*, vol. 56 (7), pp. 1–20, 2009.

[7] F. Gomez-Estern, C. Canudas-de-Wit, and F. R. Rubio, "Adaptive delta modulation in networked controlled systems with bounded disturbances," *IEEE Transaction on Automatic Control*, vol. 56 (1), pp. 129–134, 2011.

[8] A. R. Teel, "Connections between Razumikhin-type theorems and the ISS nonlinear small gain theorem," *IEEE Transactions on Automatic Control*, vol. 43 (7), pp. 960–964, 1998.

[9] K. E. Arzen, "A simple event-based PID controller," in *IFAC Congress*, 1999, pp. 423–428.

[10] J. Lunze and D. Lehmann, "A state-feedback approach to event-based control," *Automatica*, vol. 46 (1), pp. 211–215, 2010.

[11] ——, "Event-based control using quantized state information," *Estimation and Control of Networked Systems*, pp. 1–6, 2010.

[12] H. K. Khalil, *Nonlinear Systems: 3rd Edition*. Prentice Hall, 2002.

[13] E. D. Sontag and Y. Wang, "New characterizations of input-to-state stability," *IEEE Transactions on Automatic Control*, vol. 41 (3), pp. 1283–1294, 1996.

[14] D. S. Laila and D. Nesic, "Lyapunov based small-gain theorem for parameterized discrete-time interconnected ISS systems," *IEEE Transactions on Automatic Control*, vol. 48 (10), pp. 1783–1788, 2004.